Chapter

Noninvasive Bladder Volume Monitoring Using Bioimpedance

Víctor Hugo Mosquera

Abstract

Due to the electrical conductivity of the urine, several bioimpedance techniques have been considered for bladder volume monitoring. This chapter shows several approaches for bladder volume estimation; among these, Global Impedance (GI), presents a high accuracy in volume estimation. Other proposed approaches are Voltage Change Ratios (VCR), Impedance Ratio Method (IRM), and Focused Impedance Method (FIM), which presents highly sensitive to changes in the conductivity, just like GI. Therefore, these approaches are not suitable for long-term monitoring of the bladder, because the conductivity of urine varies with health status and diet. The proposal FIM-IE presents a low sensibility to the conductivity uncertainty; being a promising technique for long-term monitoring of the bladder and would support the assisted bladder emptying process.

Keywords: bioimpedance, bladder volume monitoring, EIT, global impedance, impedance ratio, voltage change ratio

1. Introduction

Electrical impedance tomography (EIT) is a noninvasive technique to obtain images of the internal conductivity of an object. The EIT systems are based on the injection of current signals and the measurement of the generated potentials at the boundary of the object under study. In EIT applications on biological tissues, the currents are usually sinusoidal, with amplitudes below 1 mA and frequencies ranging from 1 kHz to 100 kHz. Once the potentials and currents are known, an image reconstruction method is used to estimate the spatial distribution of the internal electrical conductivity of the analyzed object [1].

The so-called vesicoureteral reflux is a pathology that is presented by the leakage of urine from the bladder to the kidneys. This pathology can generate chronic renal failure, urinary tract and kidney infections, nephrotic syndrome, and scarring of the kidneys, among others. For this reason, the EIT seeks to monitor the bladder volume and support the diagnosis of this pathology [2]. It is the case of Li and colleagues [3], who designed an EIT system based on 16 electrodes, with a frequency range from 0 to 12.5 MHz; this system monitors the distribution of impedance in the bladder, and so establishes a close relationship between the bladder volume and estimated conductivity in healthy patients. On the other hand, Schlebusch and collaborators [4–6], with the aim of assist

to paraplegic patients, which present decreased bladder volume sensation due to damage to their neuronal structures, and used the EIT to monitor the bladder volume.

This chapter presents several bioimpedance indexes for bladder size monitoring, such as Global Impedance (GI), Voltage Change Ratio (VCR), and Impedance Ratio Method (IRM), which show promising results in bladder volume estimation, with the limitation that they are highly sensitive to urine conductivity. On the other hand, methods based on Focused Impedance Measurement (FIM) are presented, which have a matrix electrode configuration, different from the classical ring arrangement of the GI, VCR, and IRM methods; this matrix arrangement allows for decreasing the sensitivity of urine conductivity in the process of bladder volume estimation.

2. Urodynamics

The study of lower urinary tract function is called urodynamics, which consists of monitoring the filling and emptying of the bladder for the diagnosis and management of lower urinary tract dysfunction. This dysfunction occurs in elderly people or those with neural disorders, such as spinal cord diseases, which generate urinary incontinence (UI), detrusor hyperactivity, and prostatic hyperplasia, pathologies that cause urinary tract infections [7, 8].

Urodynamics is currently performed by means of filling cytometry, pressure-flow studies, uroflowmetry, and electromyography [9]. Cystometry is an invasive ambulatory technique that is performed by medical professionals in a Urology Unit. For this technique, a small amount of liquid at room temperature is injected through a catheter and then another equal amount of warm liquid; the patient indicates when the sensation of urination begins; when the bladder is full the patient proceeds to empty the bladder; finally, the catheter is removed from the urinary tract. During this procedure, the pressure in the bladder is measured by a cytometer [8, 10]. On the other hand, the pressure-flow study allows analysis of bladder and detrusor pressure; to determine urinary tract obstructions and alterations in detrusor contraction. This technique involves the use of a probe inside the patient's urethra to measure the detrusor pressure, so it must be performed by trained personnel [10]. Electromyography is an electrophysiological test that measures muscle activity simultaneously with cystometry. This technique seeks to detect striated muscle activity and evaluates nerve integrity, location, and severity of the lesion [10].

Another method is uroflowmetry, which measures external urine flow per unit time (Q ml/s). This is a noninvasive technique for measuring urinary flow. The patient voids the bladder into a flowmeter when he/she has the sensation of urination. This measurement reflects the kinetics of detrusor contraction. This method cannot be used as the only alternative for the diagnosis of urinary tract pathologies [7, 8, 10].

Invasive methods of urodynamic studies can cause irritation of the urethra or bladder from catheter insertion, urethral bleeding or bloody urination, infection through the catheter, urethral fistula at catheter placement, and bladder wall rupture at catheter placement [10].

EIT is a noninvasive, radiation-free clinical monitoring technique that has been investigated for many years and has shown promising results [1]. EIT measures the spatial distribution of conductivity by injecting alternating current through electrodes located at the boundary of the body under study; the voltage generated by the injected current is measured by the electrodes at the boundary; these voltages allow the estimation of the conductivity distribution and are mapped to an image with the help

of a reconstruction algorithm [11]. In addition, several low-cost EIT systems have been proposed for biomedical applications with high performance [12]. Therefore, this technique is a promising alternative for the diagnosis and monitoring of biological tissues and fluids since they present differences in their dielectric properties.

In bladder volume monitoring, EIT presents many advances that have made it possible to establish a correlation between urine conductivity and bladder volume using the Global Impedance Index (GI) [4], which is calculated from the pixels of the EIT image reconstruction. On the other hand, there are indices based on bioimpedance measurements that do not require image reconstruction algorithms to estimate bladder volumes, such as the IRM (Impedance Ratio Method) [6], VCR (Voltage Change Ratio) [13], and MVCR (Modified Voltage Change Ratio) [7], which, like GI, present a correlation between bioimpedance measurements and bladder volume. The aforementioned methods are highly sensitive to the change in urine conductivity, which occurs due to infections or the patient's diet, so volume estimation with these methods cannot be applied in the long term. For this reason, a method based on global focused impedance (FIM) is proposed in Ref. [7] that allows the estimation of bladder volume independently of urine conductivity, which allows long-term monitoring.

Methods based on bioimpedance measurements are a very good alternative for bladder volume monitoring because they require low-cost equipment and are noninvasive. Considering that GI indices, MRI, VCR, and MVCR are sensitive to urine conductivity, they may also be promising in the study of urinary tract alterations due to infections.

3. Electrical impedance tomography

Figure 1 presents the concept of the EIT, which consists of applying currents (I) on a set of electrodes connected to the boundary ($\partial\Omega$) of a body (Ω); subsequently, the resulting voltages (V) are measured on the remaining electrodes. The mathematical background of the EIT is explained in Ref. [7]; where Maxwell equations and the Faraday and Ampere laws are formulated in the differential form to define the relationship between the admittivity (γ) and the potential on the electrodes (φ) (Eq. 1).

$$\nabla \cdot (\gamma \nabla \varphi) = 0 \tag{1}$$

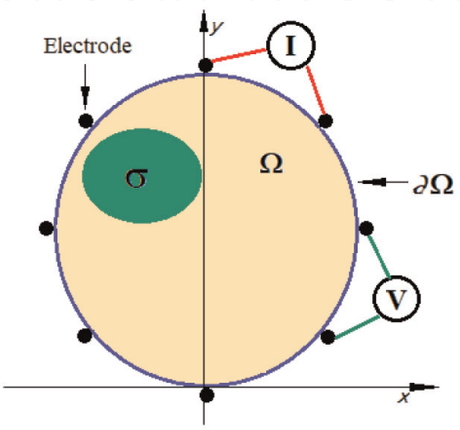

Figure 1.
Conductivity changes detection with EIT.

γ is a complex value $\gamma = \sigma + j\omega\varepsilon$, where σ represents the conductivity $i \triangleq \sqrt{-1}$ is the imaginary unit, ω denotes the angular frequency, and ε is the permittivity. This equation describes the electrical potential inside. Whenever Ω is stimulated with low-frequency currents ($\omega \approx 0$), the following EIT equation is obtained:

$$\nabla \cdot (\sigma \nabla \varphi) = 0 \tag{2}$$

The nonlinear partial differential Eq. 2 has infinite solutions. Particular solutions are obtained by applying either the Dirichlet or Neumann conditions. The former is used when voltages are applied to the boundary electrodes:

$$\varphi(x_i) = v_i \; i = 1, 2, \ldots, m \tag{3}$$

where x_i is a point on $\partial\Omega$ that indicates the position of the electrode i, v_i is the voltage applied to such electrode and m is the total number of electrodes. Neumann conditions are used when currents are injected and drained through the surface electrodes. In such a case:

$$\sigma \nabla \varphi(x_i) \cdot \vec{n} = I_i \; i = 1, 2, \ldots, m \tag{4}$$

where $\vec{n}$ is a unitary vector perpendicular to $\partial\Omega$ in x_i. I_i is the current density through the electrode i and it is positive for the injecting electrode and negative for the draining electrode. Additionally, Kirchoff's current law must be satisfied:

$$\sum_{i=1}^{m} I_i = 0 \tag{5}$$

The solution to the EIT problem is divided into two parts: i) estimate the potentials on the boundary knowing the injected current and assuming a conductivity distribution, this part is called forward problem, and ii) assess the conductivity distribution knowing the injected currents and the measured potentials or inverse problem (**Figure 2**). The forward and inverse problems are detailed below.

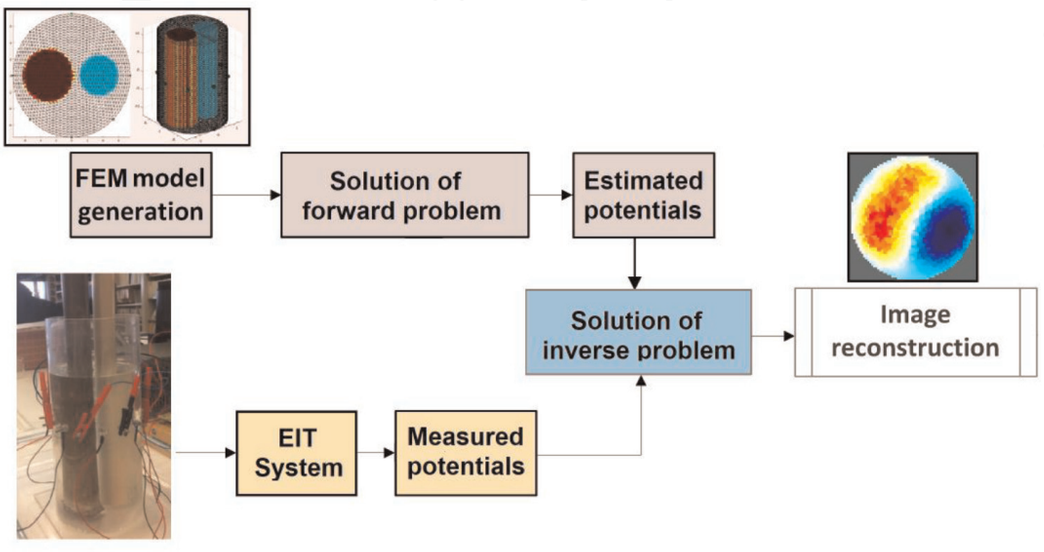

Figure 2.
EIT image reconstruction.

3.1. Forward problem

The forward problem can be solved analytically or numerically. The analytical methods are preferable as computation time is reduced; however, their usage is limited to a few idealized geometries [8]. For numerical solutions, the governing equation is discretized using the finite elements method (FEM) or the generalized FEM (GFEM) [9]. For general geometries and inhomogeneous materials, FEM is well suited to solve the forward problem and is the most used in EIT [10]. In EIT, the approach based on FEM consists of dividing Ω into a finite number of regions of constant conductivity. A relation can be obtained between the voltage measurements on the boundary and the conductivity of such regions (Eq. 6) [11, 12].

$$\Phi = J\sigma \tag{6}$$

where $\boldsymbol{J}$ is known as the sensitivity matrix or Jacobian matrix, which relates the vector of voltage measurements (Φ) with the vector of conductivities ($\boldsymbol{\sigma}$). If $\boldsymbol{\sigma}$ and $\boldsymbol{J}$ are known. Then, the estimation of Φis simple. Considering the variety of methods available in EIDORS (*Electrical Impedance Tomography and Diffuse Optical Tomography Reconstruction Software*).

3.2. Inverse problem

The inverse problem seeks to obtain the conductivity distribution using the potential on the electrodes and the injected currents. To solve the inverse problem is necessary to use a forward model to minimize the difference between the potentials estimated and measured on the boundary (**Figure 2**). There are several approaches to solve the inverse problem, which is ill-posed and is based on linearization and regularization [8]. The conductivity estimation obtained from 3.2 is:

$$J^{T}\Phi = J^{T}J\sigma \tag{7}$$

$$\sigma = \left(JJ^{T}\right)^{-1}J^{T}\Phi \tag{8}$$

The matrix (JJ^T) is ill-conditioned. The best way to solve this problem is to use regularization techniques [13], which are necessary to obtain a unique solution from an ill-posed EIT problem [14]. Additionally, a regularized solution to the inverse problem improves the reconstructed image quality [15, 16]. For these reasons, many regularization methods, such as Tikhonov [17, 18], Laplace [19], Total Variation [20], Noser [21], Helmholtz-Type [12], projection error propagation-based [15], have been proposed.

4. Volume estimation with bioimpedance

This section presents the GI (Global Impedance), FIM (Focused Impedance Measurement), IRM (Impedance Ratio Method), and VCR (Voltage Change Ratio) techniques, which have been recently proposed for volume estimation in medical applications. GI is defined as the sum of the pixels of an image and as a consequence, it requires to solve the EIT inverse problem. On other hand, the FIM approach does not need the reconstruction matrix; the potential variation is enough to estimate volume.

FIM estimates the impedance of the region of interest by means of two potential measurements mutually perpendicular giving a higher sensitivity in the central region compared to its surroundings [22]. Similar to FIM method, IRM and VCR do not require an image reconstruction algorithm. IRM, proposed in Ref. [6], estimates the volume estimation of an object employing three impedance measurements. On the other hand, VCR requires two voltage measures to estimate the volume [23], although the robustness against the uncertainty of conductivity has not been analyzed. The GI, FIM, IRM, and VCR are explained below.

4.1. Global impedance index

The GI approach is based on reconstructed images of differential EIT (dEIT) in which homogeneous ($\boldsymbol{v_h}$) and nonhomogeneous ($\boldsymbol{v_{nh}^f}$) vector measurements are taken. The superscript $\boldsymbol{f}$, which ranges from 1 to $\boldsymbol{N_f}$, indicates the frame. N is the number of voltage measures per frame and is hence the number of elements of vectors $\boldsymbol{v_h}$ and $\boldsymbol{v_{nh}^f}$. Differences between $\boldsymbol{v_h}$ and $\boldsymbol{v_{nh}^f}$ are used in an EIT reconstruction algorithm to calculate changes in the conductivity inside the object under study [5, 24]. Hence, variations in the potential for any frame f are calculated using the following operation:

$$\Delta \mathbf{v^f(k)} = \frac{\mathbf{v_{nh}^f(k)} - \mathbf{v_h(k)}}{\mathbf{v_h(k)}}, \mathbf{k} = \mathbf{1, 2, \ldots N} \tag{9}$$

where $\boldsymbol{\Delta v^f(k)}$, $\boldsymbol{v_{nh}^f(k)}$ and $\boldsymbol{v_h(k)}$ are the k-th elements of the vectors $\boldsymbol{\Delta v^f}$, $\boldsymbol{v_{nh}^f}$ and $\boldsymbol{v_h}$, respectively. To solve the pixel conductivity vector $\boldsymbol{I_f}$, the matrix $\boldsymbol{R^f}$ must be calculated using a differential EIT reconstruction algorithm. $\boldsymbol{R^f}$ has M rows and N columns (M, number of pixels of the conductivity image). Hence, the vectors $\boldsymbol{I^f}$ and $\boldsymbol{\Delta v^f}$ are related by the equation $\boldsymbol{I^f = R^f \Delta v^f}$. GI of dimensionless units is calculated by adding the values of all pixels of $\boldsymbol{I^f}$ for each frame as follows (Eq. 10):

$$\mathbf{GI} = \sum_{\mathbf{f=1}}^{\mathbf{N_f}} \sum_{\mathbf{k=1}}^{\mathbf{N}} \mathbf{I^f} \tag{10}$$

4.2. Focused impedance measurement (FIM)

FIM Method is a technique of impedance measurement that can localize a zone of interest in a volume, eliminating the effects of neighboring regions and using 8, 6, or 4 electrodes [25–27]. FIM shows promising results in gastric monitoring [28], breast tumors [29], and lung ventilation [21]. We propose a modification of the FIM approach using eight electrodes; the classical FIM and modified FIM are explained then.

4.2.1 Classic FIM method

Tetrapolar FIM's are based on the sum of independent measurements of mutually perpendicular and concentric potentials. This is done to detect changes that are generated by the injected current on the equipotential lines inside the object under study. Saha and collaborators [30] show that changes in the conductivity/impedance of the

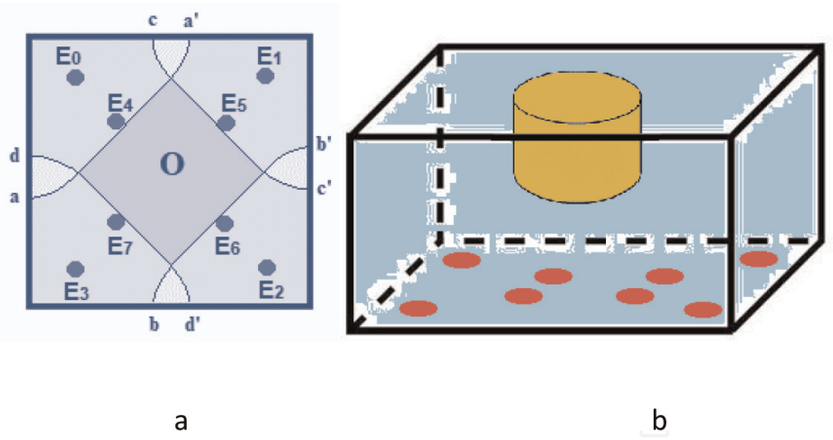

Figure 3.
a) Focused area in an 8-Electrodes FIM arrangement and b) Placement of electrodes on the bladder phantom.

object under study lead to proportional differences in electrical potential between equipotential lines. This assumption remains valid for a constant injected current. The arrangement of electrodes for FIM is shown in **Figure 3**.

When the current is injected through the E0 and E2 electrodes, equipotential lines are represented as $\boldsymbol{a}-\boldsymbol{a}'$ and $\boldsymbol{b}-\boldsymbol{b}'$. Similarly, when current is injected through the E_1 and E_3 electrodes, then the equipotential lines are represented as $\boldsymbol{c}-\boldsymbol{c}'$ and $\boldsymbol{d}-\boldsymbol{d}'$. These potentials are measured on electrodes E_4, E_5, E_6, and E_7, and the focused area O is defined for equipotential lines [31]. Changes in potential are estimated relative to the reference measure $\boldsymbol{P}_{ref}$, which is the potential when there is no object in the region **O** of **Figure 3**. In this case, the conductivity is homogeneous throughout the cross-section under study. $\boldsymbol{P}_{ref}$ is calculated using Eq. 11 as follows:

$$\mathbf{P_{ref}} = \mathbf{P}^{\mathbf{0}}_{\mathbf{4,6}} + \mathbf{P}^{\mathbf{0}}_{\mathbf{5,7}} \tag{11}$$

$\boldsymbol{P}^{\mathbf{0}}_{\mathbf{4,6}}$ is the difference in potential between the electrodes E_4 and E_5 for the homogeneous configuration (indicated with the superscript o). Similarly, $\boldsymbol{P}^{\mathbf{0}}_{\mathbf{5,7}}$ is the difference in potential between the electrodes E_5 and E_7. Hence, given a conductivity change in region O (**Figure 3**), the potential is defined in Eq. 12 as follows:

$$\mathbf{P} = \mathbf{P_{4,6}} + \mathbf{P_{5,7}} \tag{12}$$

	Injection	Measurement	
Potentials on internal electrodes	E_0-E_1	$\boldsymbol{P}_{4,5}$	$\boldsymbol{P}_{5,6}$
	E_1-E_2	$\boldsymbol{P}'_{5,6}$	$\boldsymbol{P}_{6,7}$
	E_4-E_5	$\boldsymbol{P}_{6,7}$	
	E_5-E_6	$\boldsymbol{P}_{4,7}$	
Potentials on external electrodes	E_4-E_5	$\boldsymbol{P}_{0,1}$	$\boldsymbol{P}_{1,2}$
	E_5-E_6	$\boldsymbol{P}'_{1,2}$	$\boldsymbol{P}_{2,3}$

Table 1.
Injection and measurement patterns for the proposed FIM approaches.

The variability of potential is then defined as:

$$\Delta \mathbf{P} = \frac{\mathbf{P} - \mathbf{P_{ref}}}{\mathbf{P_{ref}}} \tag{13}$$

The opposite pattern for injection and measurement using the classic FIM approach has been applied in previous studies [32], with promissory results.

4.2.2 Modified FIM method

The modified FIM approach [32] employs adjacent patterns for injection and measurement, using the same electrode arrangement of FIM classic. The electrodes were divided into externals (E_0, E_1, E_2, and E_3) and internals (E_4, E_5, E_6, and E_7) according to the configuration presented in **Figure 3**. **Table 1** shows the injection and measurement electrodes used for the two proposed FIM approaches. In the first proposed FIM approach, FIM-I (I, internal), the variable P of Eq. 13 was equal to $\boldsymbol{P_{int}}$, which is calculated as $\boldsymbol{P_{int}} = \boldsymbol{P_{4,5}} + \boldsymbol{P_{5,6}} + \boldsymbol{P'_{5,6}} + \boldsymbol{P_{6,7}}$. In the second proposed approach, FIM-IE (IE, Internal-External), $\boldsymbol{P} = \boldsymbol{P_{int}} + \boldsymbol{P_{ext}}$ with $\boldsymbol{P_{ext}} = \boldsymbol{P_{0,1}} + \boldsymbol{P'_{1,2}} + \boldsymbol{P_{1,2}} + \boldsymbol{P_{2,3}}$ and $\boldsymbol{P_{int}}$ as for FIM-I. In the previously described FIM-4 approach [32], variable $\boldsymbol{P_{int}} = \boldsymbol{P_{4,7}} + \boldsymbol{P_{6,7}}$. As indicated in **Table 1**, FIM-I requires two injections of current and four measures of voltage, whereas FIM-IE requires four injections of current and eight measures of voltage. In contrast, classic FIM-4 requires two injections of current and two measures of voltage. Pref for each approach is defined as $\boldsymbol{P}$.

4.3. Impedance ratio method (IRM)

IRM relates volume with impedance change. This technique searches the volume estimation robustness against the conductivity variability of the object under study. The three tetrapolar measurements required to calculate the impedance ratio are presented in **Figure 4** [22]. The frontal measurement is used to calculate $Z_f = V_f/I_f$, the backward measurement defines $Z_b = V_b/I_b$, and the side measurement determines $Z_s = V_s/I_s$. The potentials and the currents are measured and injected on boundary electrodes, which are placed in a ring arrangement. The measurements proposed in Ref. [22] present higher sensibility of impedance variations; assuming that the object under study must be close to the electrodes, being that the current densities are the biggest in the vicinity of these. Therefore, the volume increase of the object implies a higher change in the sensitivity of impedance measurements. Eq. 14 defines the IRM.

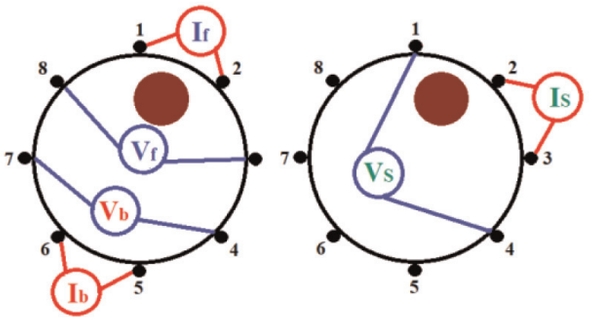

Figure 4.
Injection and measurement of signals for IRM.

$$\mathbf{IRM} = \frac{\mathbf{Z_s} - \mathbf{Z_f}}{\mathbf{Z_b} - \mathbf{Z_f}} \tag{14}$$

4.4. Voltage change ratio (VCR)

VCR [23] associates the voltage change with the volume of the object under study. This is calculated by considering a reference measurement (V_0), which is obtained when the object studied has the lowest volume. Other potential measurements (V) are taken during the increasing volume to determine the VCR (Eq. 15).

$$\mathbf{VCR} = \frac{|\mathbf{V} - \mathbf{V_0}|}{\mathbf{V_0}} \tag{15}$$

The electric potentials are measured by considering the electrode configuration shown in **Figure 5**.

VCR index uses two voltage measurements only, one reference and the other to determine the change in volume; to have redundant voltage measurements, the modified VCR (MVCR) is proposed for Ref. [32]. The MVCR requires 8 voltage measurements, as indicated in **Figure 6**. The MVCR is calculated using Eq. 16.

$$\mathbf{MVCR} = \frac{\sum_{i=8}^{8} \frac{|V_i - V_0|}{V_0}}{\mathbf{n}} \tag{16}$$

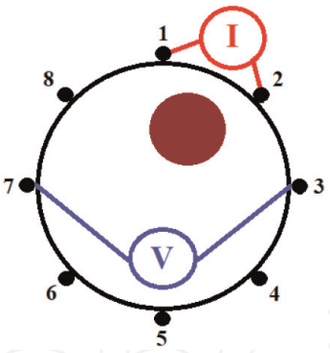

Figure 5.
Injection and measurement of signals for VCR.

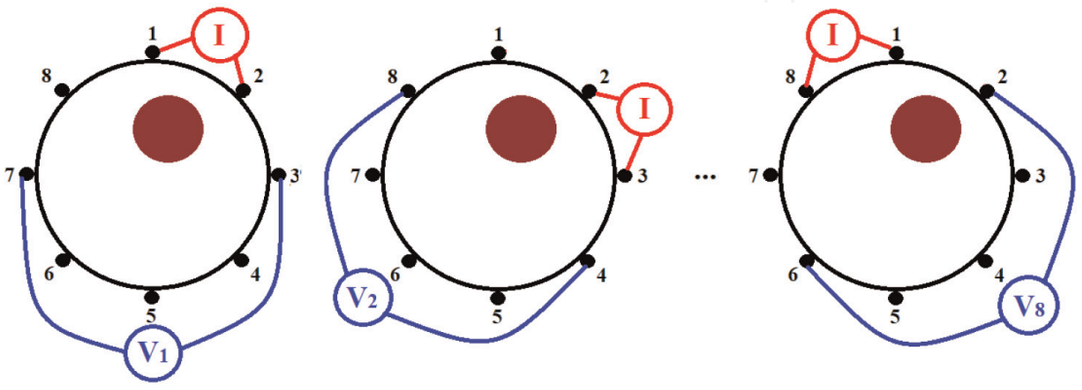

Figure 6.
Injection and measurement of signals for MVCR.

where n is the number of voltage measurements and V_0 is the reference voltage obtained when the current is injected by electrodes 1 and 2 and the studied object has the lowest volume.

5. Results of noninvasive bladder volume monitoring

GI, VCR, MVCR, MVCR, MVCR, IRM, FIM, FIM-I, and FIM-IE indices were employed for *in vitro* experiments to estimate bladder volume employing a bioimpedance measurement system previously designed in Ref. [33, 34], the results of the volume behavior are detailed below.

5.1. Sensitivity of approaches for volume estimation

The sensitivity distribution of an impedance measurement determines the impedance change caused by a given change in conductivity distribution. The sensitivity distribution also establishes the impedance contribution of each region within the area under study. The sensitivity map is the superposition of all the sensitivity distributions corresponding to each measurement. Based on Geselowitz's theorem [35], a study of sensitivity maps for the FIM, GI, VCR, and IRM approaches was performed.

Figure 7 shows that the region center of GI approach has a very low sensitivity, near to zero (represented by white color); on the other hand, the IRM, VCR, and MVCR approaches show a negative sensitivity (blue color). Considering the sensitivity maps, these indices could have the best performance if the object under study is placed near the electrodes, where the sensitivity is high (dark red color).

The sensitivity maps for the approaches based on FIM are generated through the FEM model of the phantom-like **Figure 3**; the green circles represent the location of the electrodes on the phantom. **Figure 8** shows the sensitivity of the approaches base

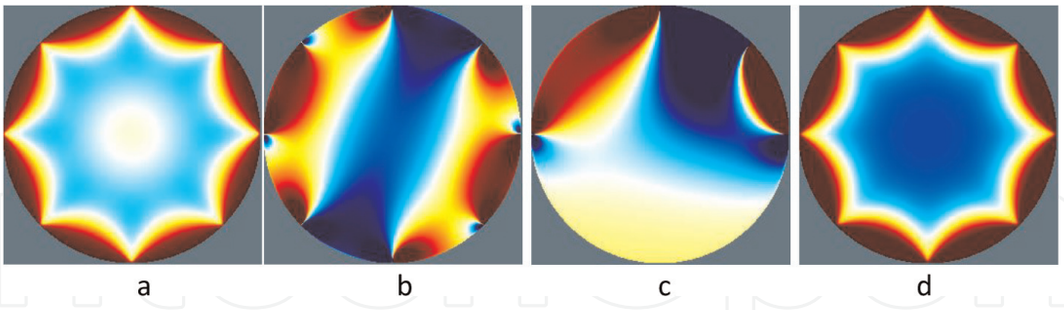

Figure 7.
Sensitivity maps of a) GI, b) IRM, c) VCR, and d) MVCR.

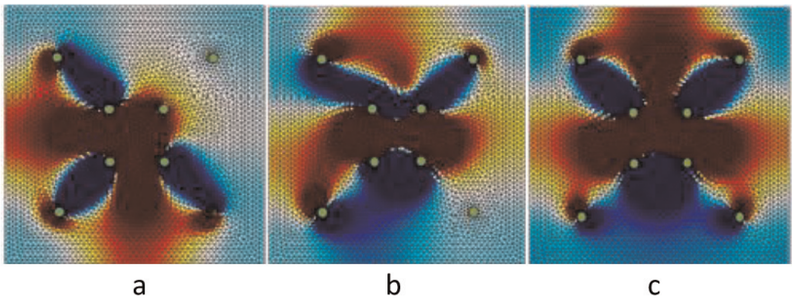

Figure 8.
Sensitivity maps of a) FIM4, b) FIM-I y and c) FIM-IE.

on FIM has greater sensitivity in the central zone than the approaches with the electrodes around the boundary. These results demonstrate that FIM-based approaches are very promising for volume estimation.

5.2. Performance of bladder volume estimation

The experiments *in vitro* to bladder volume estimation showed a linear correlation between abdominal electrical impedance and bladder volume. In Ref. [36], it is evident the linear correlation of GI index with bladder volume. On the other hand, in [mosquera20] the linear relationship positive between GI and volume was confirmed. It was also found that the GI index shows low sensitivity to measurement noise.

On the other hand, the approaches for volume estimation that do not require image reconstruction algorithms show the next results:

- The IRM in *in vitro* experiments does not correlate positively or negatively with the volume [32]. This is because when the object under study is symmetrically located with respect to the electrodes, the front, rear, and side voltages are the same, and as a consequence, the IRM becomes a quotient of noises. This fact makes IRM unsuitable for bladder volume estimation.

- The VCR in Refs. [23, 32] evidence that the median values of the VCR measurements significantly differ for the volume. Also, VCR has a positive correlation with human bladder monitoring. Furthermore.

- The MVCR is an extension of VCR that uses eight voltage measurements to improve robustness against noise, as is evidenced in Ref. [32]. Like VCR, MVCR leads to significant differences in the volume measurement.

The results *in vitro* show that GI, VCR, and MVCR are suitable approaches for volume monitoring when the conductivity of the object under study is unknown but constant. VCR has the highest sensitivity to volume variation, while MVCR had the highest noise robustness. Both VCR and MVCR are easier to implement than GI because they do not require an image reconstruction algorithm.

The studies show that when the volume remains constant, but the conductivity varies, the VCR and MVCR estimates also vary, making it impossible to distinguish between changes in volume and changes in conductivity. GI suffers from the same problem as VCR and MVCR because it is calculated as the sum of the conductivity pixels of an image; as a consequence, a large object with moderate conductivity can have a similar GI as a medium object with high conductivity. The bioimpedance approaches presented in this chapter detect changes in volume when the conductivity of the object under study remains constant. Furthermore, these methods require less computational effort than the GI approach, which is based on differential EIT and as consequence requires to solve the inverse problem.

The FIM-4 approach was proposed in a previous study [22] and comprises two mutually orthogonal tetrapolar measurements to estimate the impedance of an object that is located below the plane formed by the electrodes. Based on FIM-4, a method for organ volume estimation was proposed [37], and it was shown that simulations that are based on finite elements give linear relationships between volumes of study objects and sensitivity, which is defined as the quotient of

impedance variation and the distance between electrodes. In addition, *in vitro* experiments demonstrated that the constant that relates volume and sensitivity depends on the conductivity of the object and on its depth with respect to the plane of electrodes. Similarly, FIM-I and FIM-4 approaches depend on the conductivity of the object under study. The experiments with FIM-IE, however, showed a strict dependence on the volume. The main difference between these three FIM approaches is the additional information required to calculate variations of electrical potential. Unlike FIM-I and FIM-4 procedures, FIM-IE is performed by injecting current and measuring the voltage on internal and external electrodes. When current is injected through internal electrodes, voltage is measured at the external electrodes, and *vice versa*.

In *in vivo* experiments it was found that the GI index shows a high variation to changes in urine conductivity [5, 23] making it a method that can be oriented to short-term monitoring. In [23] shows a significantly enhances the sensitivity of the measurement with VCR index, suggesting a better protocol to maximize the value of electrical impedance in monitoring the accumulation of bladder urine.

Each of the present bioimpedance approaches for estimating bladder volumes *in vivo* requires a calibration procedure that begins by emptying the patient's bladder and then using urodynamics to relate bladder volumes to the bioimpedance variable. The resulting equations relate measurements with volumes but are only valid when urine conductivity is equal to that during the calibration phase. Because urine conductivity varies physiologically, it is important to use bioimpedance approaches for which measured variables are independent of urine conductivity. The FIM-IE approach meets these criteria.

The results obtained in studies lead us to conclude that the proposed FIM-IE approach has low sensitivity against conductivity uncertainty, allowing volume monitoring to long-term; contrary to the performance shown by VCR, IRM, and GI indices, which have a high sensibility to conductivity uncertainty as is reported in Refs. [6, 23, 31, 32].

6. Conclusions

Since the methods currently used (cytometry, pressure-flow studies, and electromyography) for urodynamic studies are invasive and can cause irritation, bleeding, infection, urethral fistula, and rupture of the urinary system [10], bioimpedance-based methods are an excellent alternative for bladder monitoring because they do not involve risks due to the use of catheters or probes in the urinary tract. On the other hand, uroflowmetry, being a noninvasive method, is not suitable for the diagnosis of urinary system pathologies [8]; therefore, the use of bioimpedance, being sensitive to urine conductivity and allowing estimation of bladder volume, is a method that could generate a diagnosis of the behavior and state of the urinary system; being a better alternative than uroflowmetry.

Unlike the VCR, MRI, and GI approaches, which are highly sensitive to conductivity changes, FIM-IE is very robust to uncertainty in this variable, making it suitable for long-term bladder volume monitoring. Therefore, FIM-IE is a promising alternative to avoid inappropriate catheterization in patients with loss of voiding sensation and the future, detect vesicoureteral reflux. On the other hand, GI, VCR, and MVCR, being highly sensitive to urine conductivity, may be promising alternatives to test urine conductivity for abnormalities due to bacteria or infections.

Acknowledgements

The authors thank the support of the research group of Automation of Universidad del Cauca (501100005682).

Author details

Víctor Hugo Mosquera
Universidad del Cauca, Popayán, Colombia

*Address all correspondence to: mosquera@unicauica.edu.co

References

[1] Harikumar R, Prabu R, Raghavan S. Electrical impedance tomography (EIT) and its medical applications: A review. International Journal of Software Computer and Engineering. 2013;**3**: 193-198

[2] Dunne E, O'Halloran M, Craven D, Puri P, Frehill P, Loughney S, et al. Detection of vesicoureteral reflux using electrical impedance tomography. IEEE Transactions on Biomedical Engineering. 2018;**66**:2279-2286

[3] Li R, Gao J, Li Y, Wu J, Zhao Z, Liu Y. Preliminary study of assessing bladder urinary volume using electrical impedance tomography. Journal of Medical and Biological Engineering. 2016;**36**:71-79

[4] Schlebusch T, Nienke S, Santos SA, Leonhardt S. Bladder volume estimation from electrical impedance tomography. In: 35th Annual International Conference of the IEEE Engineering in Medicine and Biology Society (EMBC). 2013

[5] Schlebusch T, Leonhardt S. Effect of electrode arrangements on bladder volume estimation by electrical impedance tomography. Journal of Physics: Conference Series. 2013

[6] Schlebusch T, Orschulik J, Malmivuo J, Leonhardt S, Leonhäuser D, Grosse J, et al. Impedance ratio method for urine conductivity - invariant estimation of bladder volume. Journal of Electrical Bioimpedance. 2019;**5**:48-54

[7] Bragos R, Rengifo C, Mosquera V. Robustness of focused and global impedance estimates of bladder volumes against uncertainty of urine conductivity. Biomedical Physics & Engineering Express. 2020;**6**(2): 045008

[8] Abelson BS, Majerus D, Sun B, Gill E, Versi M, Damaser, Ambulatory urodynamic monitoring: State of the art and future directions, Nature Reviews. Urology. 2019;**16**(5):291-301

[9] Li Y, Peng Y, Yang X, Lu S, Gao J, Lin C, et al. Analysis of measurement electrode location in bladder urine monitoring using electrical impedance. Biomedical Engineering Online. 2019;**18**: 34

[10] Salazar MP. El estudio urodinámico, Uroligía Colombiana. 2014;**23**(2):128-1308

[11] Holder DS. Electrical Impedance Tomography: Methods, History and Applications. Institute of Physics Publishing. Boca Raton: CRC Press; 2004

[12] Simini F, Bertemes-Filho P. Bioimpedance in Biomedical Applications and Research. New York: Springer; 2018

[13] Lu L, Liu L, Hu C. Analysis of the electrical impedance tomography algorithm based on finite element method and Tikhonov regularization. In: 2014 International Conference on Wavelet Analysis and Pattern Recognition. 2014

[14] Kantartzis P, Liatsis P. On sparse forward solutions in non-stationary domains for the EIT imaging problem. Annual International Conference of the IEEE Engineering in Medicine and Biology Society. 2011

[15] Zaravi S, Amirfattahi R, Vahdat BV. Expanding 2D block method in two direction by a new formula in EIT. In: 23rd Iranian Conference on Electrical Engineering. 2015

[16] Zaravi S, Amirfattahi R, Vahdat BV, Hassanipour A. Improving 2D block method in electrical impedance tomography. In: 22nd Iranian Conference on Biomedical Engineering (ICBME). 2015

[17] Romano D, Pisa S, Piuzzi E. Implementation of the Newton-Raphson and admittance methods for EIT. International Journal of Bioelectromagnetism. 2010;**12**:12-20

[18] Lionheart WRB. EIT reconstruction algorithms: Pitfalls, challenges and recent developments. Physiological Measurement. 2004;**25**:125

[19] Bera TK, Biswas SK, Rajan K, Nagaraju J. Image reconstruction in Electrical Impedance Tomography (EIT) with projection error propagationbased regularization (PEPR): a practical phantom study. International Conference on Advanced Computing, Networking and Security. 2011

[20] Bera TK, Nagaraju J. A study of practical biological phantoms with simple instrumentation for electrical impedance tomography (\textsc{EIT}). In: de Instrumentation and Measurement Technology Conference, 2009. I2MTC '09. IEEE; 2009

[21] Jin B, Maass P. An analysis of electrical impedance tomography with applications to Tikhonov regularization. ESAIM: Control, Optimisation and Calculus of Variations. 2012;**18**: 1027-1048

[22] Graham BM, Adler A. Electrode placement configurations for 3D EIT. Physiological Measurement. 2007; **28**:S29

[23] Tawil DS, Rye D, Velonaki M. Improved image reconstruction for an EIT-based sensitive skin with multiple internal electrodes. IEEE Transactions on Robotics. 2011;**27**:425-435

[24] Borsic A, Graham BM, Adler A, Lionheart WRB. In vivo impedance imaging with total variation regularization. IEEE Transactions on Medical Imaging. 2009;**29**:44-54

[25] Rabbani KS, Sarker M, Akond MHR, Akter T. Focused impedance measurement (FIM): A new technique with improved zone localization. Annals of the New York Academy of Sciences. 1999;**873**:408-420

[26] Leonhardt S, Cordes A, Plewa H, Pikkemaat R, Soljanik I, Moehring K, et al. Electric impedance tomography for monitoring volume and size of the urinary bladder. Biomedizinische Technik. 2011;**56**:301-307

[27] Schlebusch T, Nienke S, Leonhäuser D, Grosse J, Leonhardt S. Optimal electrode positions to determine bladder volume by bioimpedance spectroscopy. Lecture Notes on Impedance Spectroscopy. 2013;**4**:67-73

[28] Rabbani KS, Karal MAS. A new four-electrode focused impedance measurement (FIM) system for physiological study. Annals of Biomedical Engineering. 2008;**36**: 1072–1077

[29] Abir AR, Rabbani KS-E. Sensitivity study for a 4-electrode focused impedance method (FIM) using finite element method analysis. Bangladesh Journal of Medical Physics. 2015;**7**

[30] Pettersen FJ, Ferdous H, Kalvøy H, Martinsen ØG, Høgetveit JO. Comparison of four different FIM configurations—A simulation study. Physiological Measurement. 2014;**35**: 1067

[31] Iquebal M, Rabbani KS-E. Correlation of liquid volume in stomach to electrical transfer impedance measurements using FIM. Bangladesh Journal of Medical Physics. 2014;**6**:66-74

[32] Al Amin A, Parvin S, Kadir MA, Tahmid T, Alam SK, Rabbani KS-E. Classification of breast tumour using electrical impedance and machine learning techniques. Physiological Measurement. 2014;**35**:965

[33] Kadir MA, Ahmed SP, Al Quaderi GD, Rahman R, Rabbani KS-E. Application of focused impedance method (FIM) to determine the volume of an object within a volume conductor. In: Proceedings of the 2013 COMSOL Conference, Bangalore, India. 2013

[34] Saha SK, Al-Quaderi GD, Rabbani KS-E. 3D sensitivity of 8-electrode FIM through experimental study in a phantom. Bangladesh Journal of Medical Physics. 2014;**6**:55-65

[35] Rabbani KS-E, Kadir MA. Possible applications of focused impedance method (FIM) in biomedical and other areas of study. Bangladesh journal of Medical Physics. 2013;**4**:67-74

[36] Mosquera VH, Arregui A, Bragós Bardia R, Rengifo CF. Implementation of a low cost prototype for electrical impedance tomography based on the integrated circuit for body composition measurement AFE4300. In: Proceedings of the 11th International Joint Conference on Biomedical Engineering Systems and Technologies (BIOSTEC 2018): January 19–21, 2018: Funchal, Madeira, Portugal. 2018

[37] He W, Ran P, Xu Z, Li B, Li S-N. A 3D visualization method for bladder filling examination based on EIT. Computational and Mathematical Methods in Medicine. 2012;**2012**:9